



# Hybrid effects of steel fiber and microfiber on the tensile behavior of ultra-high performance concrete



Su-Tae Kang<sup>a</sup>, Jeong-Il Choi<sup>b</sup>, Kyung-Taek Koh<sup>c</sup>, Kang Seok Lee<sup>b</sup>, Bang Yeon Lee<sup>b,\*</sup>

<sup>a</sup> Department of Civil Engineering, Daegu University, 201 Daegu-dae-ro, Jillyang, Gyeongsan, Gyeongbuk 38453, Republic of Korea

<sup>b</sup> School of Architecture, Chonnam National University, 77 Yongbong-ro, Buk-gu, Gwangju 61186, Republic of Korea

<sup>c</sup> Korea Institute of Construction Technology, 293 Goyang-daero, Ilsanseo-gu, Goyang-si, Gyeonggi-do 10223, Republic of Korea

## ARTICLE INFO

### Article history:

Available online 2 March 2016

### Keywords:

Compressive strength  
Hybrid fiber  
Microfiber  
Steel fiber  
Tensile behavior  
UHPC

## ABSTRACT

Ultra-high performance concrete (UHPC) has ultra-high material performance including high strength and high flowability. However, its tensile strain capacity is generally lower than that of high ductile cementitious composite. This study experimentally investigated the effect of hybrid combinations of straight 0.2 mm diameter steel fiber and various microfibers on the mechanical properties of UHPC. Four types of hybrid fiber reinforced UHPCs including steel, basalt fibers, polyvinyl-alcohol, and polyethylene fibers were designed and then compressive strength, density, and tensile behavior were investigated. Test results showed that combining a synthetic fiber with high strength, such as PE fiber, and steel fiber can improve the tensile behavior of UHPC and basalt fiber was effective for improving the tensile strength of UHPC.

© 2016 Elsevier Ltd. All rights reserved.

## 1. Introduction

Recently, the repair and rehabilitation of aged and deteriorated structures have become an important issue in the fields of architecture and civil engineering. According to the 2009 Report Card for America's Infrastructure presented at the National Press Club, the overall grade for American infrastructures was a "D". In addition, the magnitude and number of natural and man-made hazards is growing. To address these issues, there is a need for technological advances that improve either the condition or performance of the members of existing structures [1]. Ultra-high performance concrete (UHPC) has been studied and developed to meet this technical demand [2–4]. According to a Federal Highway Administration Report [5], since the first UHPC bridge was constructed, more than 90 UHPC bridges have been constructed in America, Australia, Austria, Croatia, France, Germany, Italy, Japan, Republic of Korea, Malaysia, Netherlands, New Zealand, and Slovenia, and recommendations on UHPC construction have been published in France, Japan, Republic of Korea, etc.

The main reason why research on UHPC is being widely performed, and UHPC is being used around the world, is due to the superior properties of UHPC. According to Association Française de Génie Civil [6], UHPC tends to have compressive strength over

150 MPa, fiber reinforcement to ensure non-brittle behavior, and a high binder ratio with special aggregates. Furthermore, UHPC tends to have a very low water content and can achieve proper rheological properties through controlling the packing density of solid ingredients and the addition of superplasticizer. However, the tensile ductility of UHPC is much lower than that of high ductile cementitious composites such as high-performance fiber reinforced cementitious composites [7–11].

To maximize the improvements possible through fiber reinforcement, a previous study reported that including two or more types of fiber can make complementary and additive contributions to performance in a concrete mix [12]. A combination of macrofiber with the diameter over 0.5 mm and microfiber with the diameter less than 0.022 mm has been demonstrated to be effective to improve the tensile behavior of concrete. This is attributed that the two types of fiber influence crack growth at different stages of the failure process [13,14]. It was also reported that a hybrid steel macrofiber and microfiber reinforced concrete showed higher strength and toughness compared with single type macrofiber reinforced concrete. This is because the microfibers induced the delay of macrocracks formation, which governs the tensile strength [15].

Straight steel fiber of 0.2 mm in diameter is generally used for UHPC [16]. Therefore, the effect of adding microfiber to UHPC may be different than the effects reported in previous studies. There has also been a lack of research on the combination of steel

\* Corresponding author. Tel.: +82 62 530 1648; fax: +82 62 530 1639.

E-mail address: [bylee@jnu.ac.kr](mailto:bylee@jnu.ac.kr) (B.Y. Lee).

fiber and microfibers in UHPC until now. This study experimentally investigated the effect of the hybrid combination of straight steel fiber of 0.2 mm diameter and microfiber on the mechanical properties of UHPC.

## 2. Materials and methods

### 2.1. Materials and mixture proportion

The mix proportion of the UHPC investigated in this study before adding fiber is listed in Table 1. It was designed to have a compressive strength of 150 MPa when it was cured in water at a temperature of  $23\text{ }^{\circ}\text{C} \pm 3\text{ }^{\circ}\text{C}$  for 28 days. The water to binder ratio was held constant at 0.2 and Type I Portland cement with the specific surface area of  $3413\text{ cm}^2/\text{g}$  and zirconia silica fume with the specific surface area of  $8\text{ m}^2/\text{g}$  were used as a binder. Zirconia silica fume was adopted to increase the strength of the UHPC by pozzolanic reaction and to fill the voids created by free water in the matrix, as well as to increase the packing density and improve flowability by introducing ball bearings between larger particles. The chemical composition of zirconia silica fume was measured using X-ray fluorescence (XRF) and is listed in Table 2. The chemical composition of zirconia silica fume is similar to that of silica fume. The specific surface of zirconia silica fume, however, is about half that of the silica fume used in cementitious mixtures [17]. A filler of pure silica composed of over 99%  $\text{SiO}_2$ , with an average diameter of  $2.2\text{ }\mu\text{m}$ , was adopted for increasing flowability and strength. The size of the filler was between that of the cement and zirconia silica fume. Therefore, it can increase the packing density, which results in low plastic viscosity and yield stress [18]. In addition, it can also fill voids, which results in an increase in strength and durability. Fine aggregate (an average particle size of  $500\text{ }\mu\text{m}$  or less) with a density of  $2.62\text{ g/cm}^3$  was used to maintain adequate stiffness and volume stability [19]. Large aggregates were excluded because those lead to higher matrix toughness, which induce less steady state cracking condition. An expansion admixture (EA) and shrinkage reducing admixture (SRA) were adopted to reduce autogenous shrinkage. Optimized amounts of superplasticizer (SP) was used to achieve high flowability, and antifoamer was included to minimize the amount of air bubbles.

Table 3 lists the contents of fibers used to investigate the effect of a hybrid combination of steel fiber and microfiber on the tensile behavior of UHPC. Total fiber volume was held constant at 1.5 vol.% in all four mixes. The S1.5 is a control mixture, in which two types of steel fibers with lengths of 19.5 mm and 16.5 mm were added into the UHPC mortar. S1.0-B0.5, S1.0-PVA0.5, and S1.0-PE0.5 are hybrid fiber UHPC reinforced by basalt fiber, polyvinyl-alcohol (PVA) fiber, and polyethylene (PE) fiber, respectively, at 33% replacement by volume. The properties of the fibers are listed in Table 4. All fibers had a round cross-section.

### 2.2. Mixing, casting, and curing of specimens

Each of the four compositions was mixed in a Hobart type mixer. Powder type ingredients, i.e. cement, zirconia silica fume, filler, fine aggregate, EA, and SRA, were added to the mixer and mixed at a mixing speed of 90 rpm (revolutions per minute) for 10 min. Water, SP, and antifoamer were added and the mixture

**Table 2**  
Chemical composition of zirconia silica fume.

Material	Chemical composition (%)						
	$\text{SiO}_2$	$\text{ZrO}_2$	$\text{CaO}$	$\text{Al}_2\text{O}_3$	$\text{Fe}_2\text{O}_3$	$\text{MgO}$	etc.
Zirconia silica fume	96.00	3.0	0.38	0.25	0.12	0.1	0.15

**Table 3**  
Fiber contents according to hybrid fiber system for UHPC.

	Fiber volume (%)				
	Steel 19.5	Steel 16.5	Basalt	PVA	PE
S1.5	1.0	0.5			
S1.0-B0.5	0.67	0.33	0.5		
S1.0-PVA0.5	0.67	0.33		0.5	
S1.0-PE0.5	0.67	0.33			0.5

**Table 4**  
Properties of fibers.

Type of fiber	Diameter ( $\mu\text{m}$ )	Length (mm)	Tensile strength (MPa)	Density ( $\text{g/cm}^3$ )	Elastic modulus (GPa)
Steel	200	16.3, 19.5	2500	7.8	200
Basalt	12	12	2100	2.65	100
PVA	40	12	1100	1.3	41
PE	12	18	2700	0.97	88

was then mixed at the same mixer speed until that the powder mixture changed into liquid, approximately 3–5 min. After the mixture became flowable, the mixture was mixed at a mixing speed of 270 rpm for about 3 min. Once a consistent mixture was reached, the steel fiber and microfiber were sequentially added, taking care to ensure uniform fiber dispersion; the mixture was then mixed for about 5 min. Finally, the mixture was mixed at a mixing speed of 90 rpm for 1 min to eliminate bubbles. After mixing, each mixture was cast into molds (six specimens for the uniaxial tension test and six 50 mm cubes for the cube compression test). The molds were covered with plastic sheets to minimize the evaporation of water and cured in air at a temperature of  $23\text{ }^{\circ}\text{C} \pm 3\text{ }^{\circ}\text{C}$  for 2 days. The molds were then removed and the hardened specimens were cured in water until 28 days at a temperature of  $23\text{ }^{\circ}\text{C} \pm 3\text{ }^{\circ}\text{C}$ .

### 2.3. Density test

The hardened densities of specimens,  $\rho$ , were calculated from Eq. (1) by measuring the weights of the specimens in air,  $W_A$ , and in water,  $W_W$  at 28 days in a saturated-surface-dry state.

$$\rho = \frac{W_A}{W_A - W_W} \times \rho_w \quad (1)$$

Here,  $\rho_w$  is the density of water ( $1\text{ g/cm}^3$ ).

### 2.4. Mechanical tests

The compressive strength was measured on cube specimens measuring  $50\text{ mm} \times 50\text{ mm} \times 50\text{ mm}$  according to ASTM

**Table 1**  
Mix proportion of UHPC (weight ratio).

Compound	Binder		w/b	Filler	Fine aggregate	EA	SRA	SP	Antifoamer
	Cement	Zirconia silica fume							
Proportion	1	0.25	0.2	0.3	1.1	0.075	0.01	0.023–0.026	0.0007

C109-07 [20]. To characterize the tensile behavior of each tension specimen, uniaxial tension tests were performed on the specimens with dimensions recommended by JSCE using an electronic universal testing machine under displacement control at a loading speed of 0.1 mm/min [7]. During the tests, the loading force and elongation were measured. In order to measure the elongation, two linear variable differential transducers were attached to both sides of the center of the tensile specimen. The gage length for each specimen was measured during the test setup, before starting the tension test to avoid errors during the calculation of the tensile strain from the deformation. The dimensions of the cross-section of specimens were 30 mm × 30 mm. Fig. 1 shows the geometry of tension specimen and the setup of test.

### 3. Results and discussion

#### 3.1. Density

Table 5 presents the hardened densities of each composite. The density of S1.5 was 2.48 g/cm<sup>3</sup>. The densities of S1.0-B0.5, S1.0-PVA0.5, and S1.0-PE0.5 were 1.6%, 2.0%, and 1.2% lower than that of S1.5, respectively. This decrease was attributed to the fact that microfiber has a lower density than steel fiber. Sometimes incorporating microfibers may cause an unexpected remarkable increase of porosity due to the formation of unintended pores. From the density test results, it was confirmed that unintentional pores were not created by the microfiber addition for the UHPC mixtures investigated here.

#### 3.2. Compressive strength

The 28 days compressive strength values of each composite are listed in Table 6. The S1.0-B0.5, S1.0-PVA0.5 and S1.0-PE0.5 showed 14.1%, 4.03% and 4.70% lower compressive strength than S1.5, respectively. Overall, these experimental observation shows that the addition of microfibers induce the decrease of compressive strength of UHPC. Although the compressive strength of S1.0-PVA0.5 and S1.0-PE0.5, which are UHPC reinforced by synthetic fiber, decreased compared to S1.5, the decrease of compressive strength is not high. From these test result, it was exhibited that hybridization with basalt fiber was more unfavorable in compressive strength than PVA or PE fibers. The tensile performance of

**Table 5**

Density of each composite.

Fiber system	Density (g/cm <sup>3</sup> )
S1.5	2.48 ± 0.054
S1.0-B0.5	2.44 ± 0.013
S1.0-PVA0.5	2.43 ± 0.016
S1.0-PE0.5	2.45 ± 0.045

**Table 6**

Compressive strength.

Mixture ID	Compressive strength (MPa)
S1.5	149 ± 6.20
S1.0-B0.5	128 ± 5.03
S1.0-PVA0.5	143 ± 4.49
S1.0-PE0.5	142 ± 2.59

each composite considering the compressive strength will be discussed in the next section.

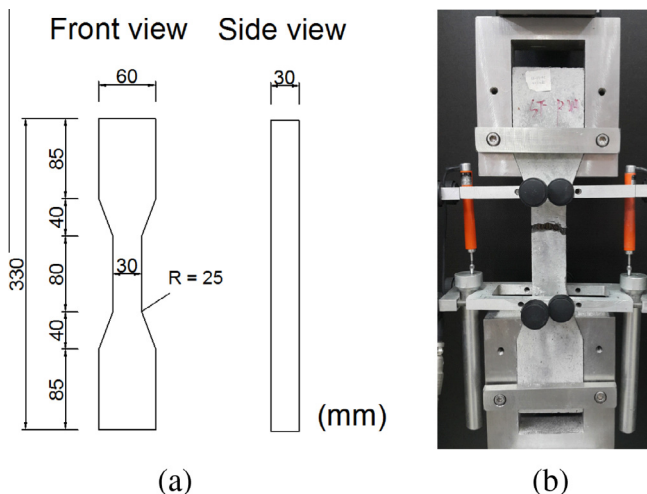
#### 3.3. Uniaxial tensile performance

Fig. 2 shows the uniaxial tensile stress curves of four kinds of UHPCs with different combinations of fiber reinforcement. As shown in Fig. 2, the tensile behavioral characteristics of most specimens are consistent with the common behavior of UHPC. That is, first cracking is followed with strain hardening behavior, reaching ultimate tensile strength; thereafter it shows strain softening behavior, which means stress loss with elongation. The growth of localized cracking appears while undergoing strain softening and finally it reaches failure.

It was found that the S1.0-PE0.5, where PE fiber was adopted instead of steel fiber for 33% of the total fiber volume, presented better tensile performance compared to S1.5, whereas the S1.0-B0.5 and S1.0-PVA0.5 indicated worse tensile performance. Three specimens of six total specimens for the S1.0-B0.5 exhibited dominant strain softening behavior even though there was strain hardening behavior for a while after drastic stress loss as soon as a first crack occurred. The strain softening behavior occurs when the stress and energy criteria were not satisfied [21]. It was observed that these specimens do not satisfy the stress criterion, i.e. the first cracking strength of the composite was higher than the ultimate tensile strength which is maximum fiber bridging stress.

Table 7 lists a comparison of the first cracking strength, ultimate tensile strength, and tensile strain capacity of each composite. The combination of fibers was found to have an influence on the first cracking strengths. The control S1.5 exhibited 9.80 MPa for the first cracking strength on average. The S1.0-B0.5 enhanced the first cracking strength by 37%. Basalt fiber proved to be beneficial in improving the first cracking strength. Unlike the other types of fibers, the basalt fiber is composed of minerals similarly to that of cementitious materials. This may result in strong chemical bonding with the cement matrix, and lead to the higher strength [22]. Although the S1.0-PVA0.5 resulted in a reduction in first cracking strength, and was 11% lower than S1.5, the S1.0-PE0.5 had 14% higher first cracking strength than S1.5.

In Table 7, ultimate tensile strength means maximum tensile stress, which simultaneously corresponds to the maximum fiber bridging stress at the crack plane if the maximum fiber bridging stress is larger than the first cracking strength. The ultimate tensile strength of S1.5 averaged 14.3 MPa. Although the ultimate tensile strength in three specimens of S1.0-B0.5 was same to the first cracking strength, the S1.0-B0.5 had a slight increment in the ultimate tensile strength, by 3%. These experimental results demonstrate that the partial replacement of steel fibers with basalt



**Fig. 1.** Uniaxial tension test: (a) the specimen geometry and (b) the uniaxial tension test setup.

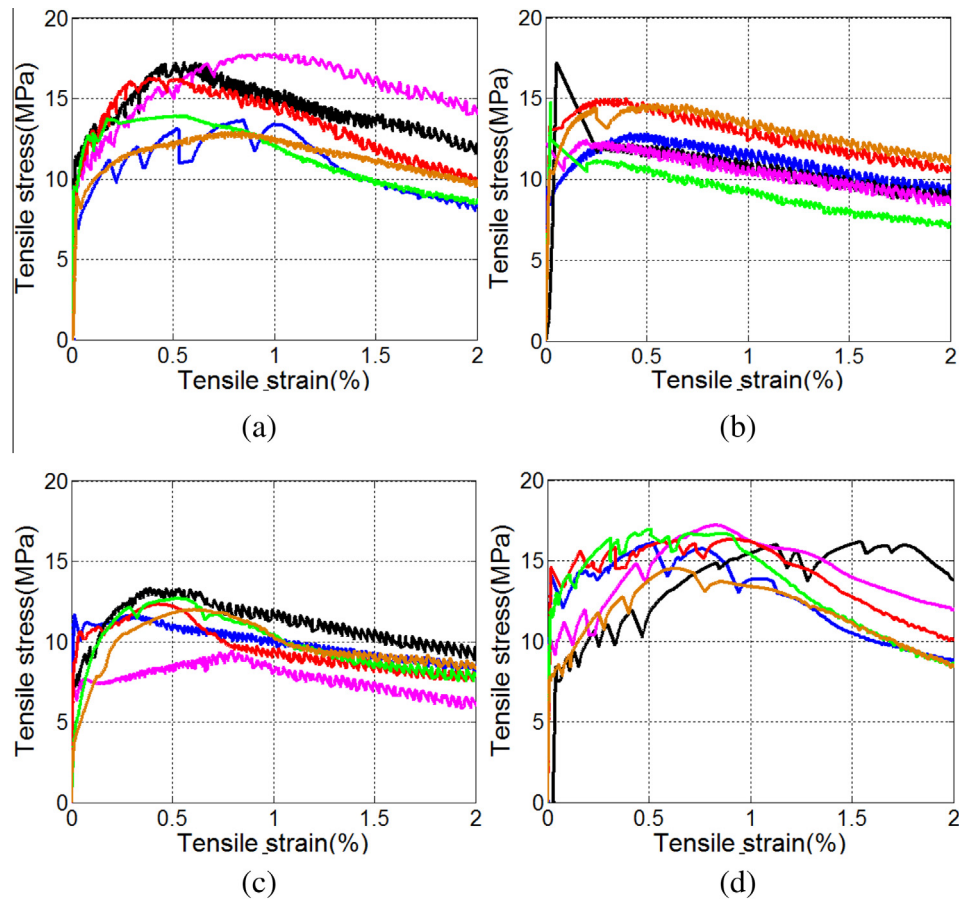


Fig. 2. Tensile stress vs. strain curve of (a) S1.5, (b) S1.0-B0.5, (c) S1.0-PVA0.5, and (d) S1.0-PE0.5.

**Table 7**  
Uniaxial tension test results.

Mixture ID	First cracking strength (MPa)	Ultimate tensile strength (MPa)	Tensile strain capacity (%)
S1.5	$9.80 \pm 1.80$	$14.30 \pm 1.83$	$0.71 \pm 0.19$
S1.0-B0.5	$13.42 \pm 2.60$	$14.74 \pm 1.32$	$0.22 \pm 0.27$
S1.0-PVA0.5	$8.71 \pm 1.57$	$11.84 \pm 1.22$	$0.58 \pm 0.15$
S1.0-PE0.5	$11.13 \pm 2.59$	$16.21 \pm 0.85$	$0.99 \pm 0.35$

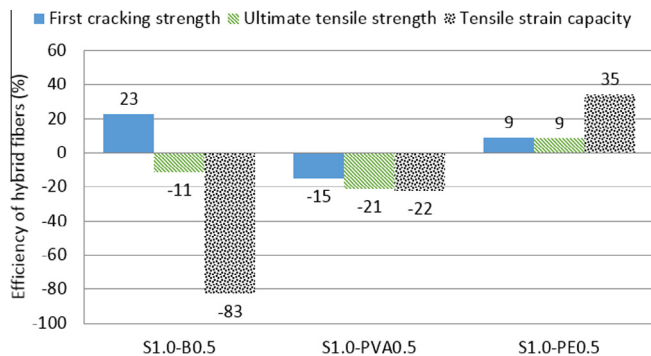


Fig. 3. Tensile performance efficiency of hybrid fiber reinforced UHPC.

fibers can improve both the first cracking strength and ultimate tensile strength of UHPC. The S1.0-PVA0.5 exhibited a 17% ultimate tensile strength reduction compared to S1.5. On the other hand, the S1.0-PE0.5 had a 13% higher ultimate tensile strength than S1.5.

Tensile strain capacity is defined as the strain corresponding to the ultimate tensile strength. The S1.5 exhibited a tensile strain capacity of 0.71% on average. Compared to the control S1.5, the S1.0-PE0.5 had 39% higher tensile strain capacity, however the S1.0-B0.5 and S1.0-PVA0.5 had 68% and 18% lower tensile strain capacity, respectively.

Fig. 3 shows the efficiency in tensile performance of hybrid fiber reinforced UHPC considering the compressive strength. The relative changes of tensile performance of S1.0-B0.5, S1.0-PVA0.5, and S1.0-PE0.5 compared to that of S1.5 were subtracted by the relative changes of compressive strength. Positive efficiency means that the increase in tensile performance is larger than the decrease in compressive strength. The S1.0-PE0.5 showed the positive efficiency on all tensile performances. On the other hand, the S1.0-PVA0.5 showed the negative efficiency on all tensile performances and the S1.0-B0.5 showed the negative efficiency on tensile performances except the first cracking strength. As shown in several earlier studies [12,13,15], it was found that incorporating microfibers can increase tensile strength as well as ductility by delaying the occurrence of macrocracking in fiber reinforced concrete as well. However, in the case of very high strength composites such as



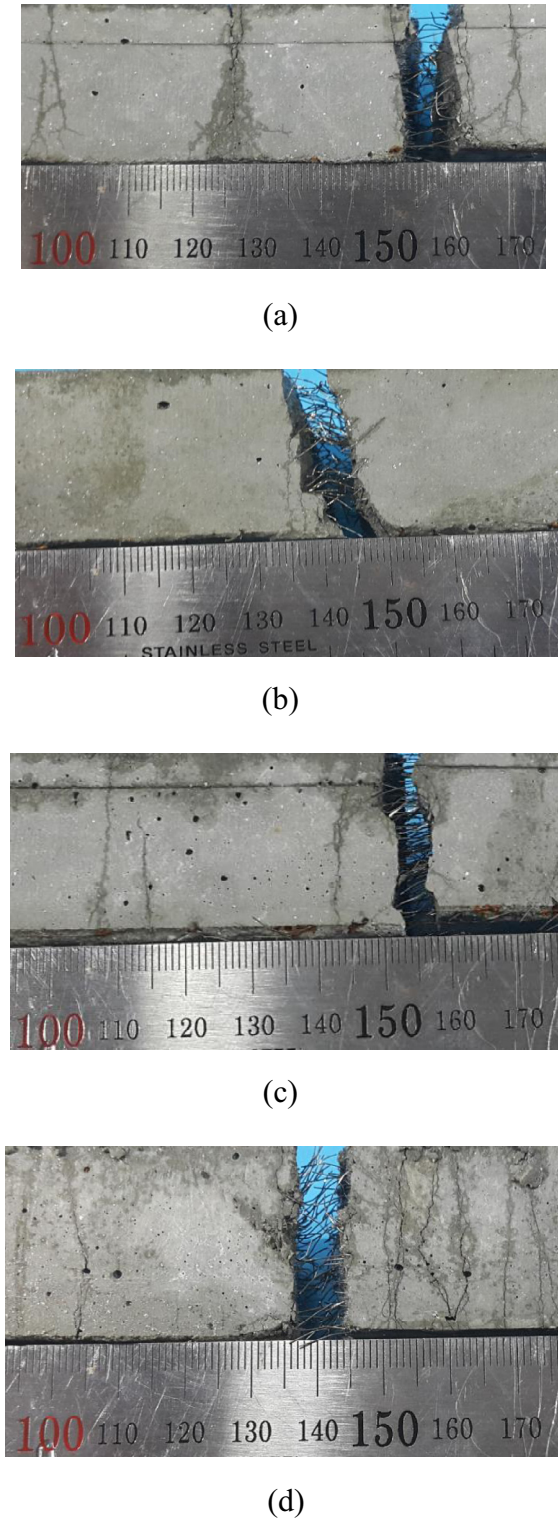


**Fig. 4.** Cracking pattern (Unit of number: mm): (a) S1.5, (b) S1.0-B0.5, (c) S1.0-PVA0.5, and (d) S1.0-PE0.5.

the UHPC studied here, the improvement in tensile performance could be obtained only when a high strength fiber like PE fiber was incorporated into the matrix.

Fig. 4 presents crack patterns observed in the specimens manufactured with four different mixtures during tensile testing. As can be seen in Fig. 4, S1.0-PE0.5 exhibited noticeable multiple cracking before final failure, however, the others didn't present clear multi-

ple cracking. One large crack was observed in the S1.0-B0.5 at failure. Representative cracks in the S1.5 as well as S1.0-PE0.5 were observed using an optical microscope after testing. Even though there was a variation in measured crack width depending on the cracking position, the crack width in the S1.5 specimen was  $54\ \mu\text{m}$  (Fig. 5). A similar crack pattern and width was observed in both the S1.0-PVA0.5 and S1.0-B0.5 specimens. On the other hand, the S1.0-PE0.5 specimen had a relatively large crack width of  $126\ \mu\text{m}$ . This observation indicates that the partial substitution of PE fiber for steel fiber enabled effective fiber bridging resistance until reaching the larger crack width, and consequently delayed localized crack growth. It also resulted in a larger crack opening at the moment of maximum fiber bridging stress.

The tensile performance of the composites was investigated with various fiber combinations of hybrid reinforcement in UHPC, and several characteristics in the tensile behavior were compared. The influence of each fiber which had been partially substituted for steel fiber could be distinguished clearly. If complementary experiments and analyses for fiber pullout behavior and fiber bridging behavior can be provided, a more comprehensive and quantitative analysis of the tensile behavior of the composites can be obtained.

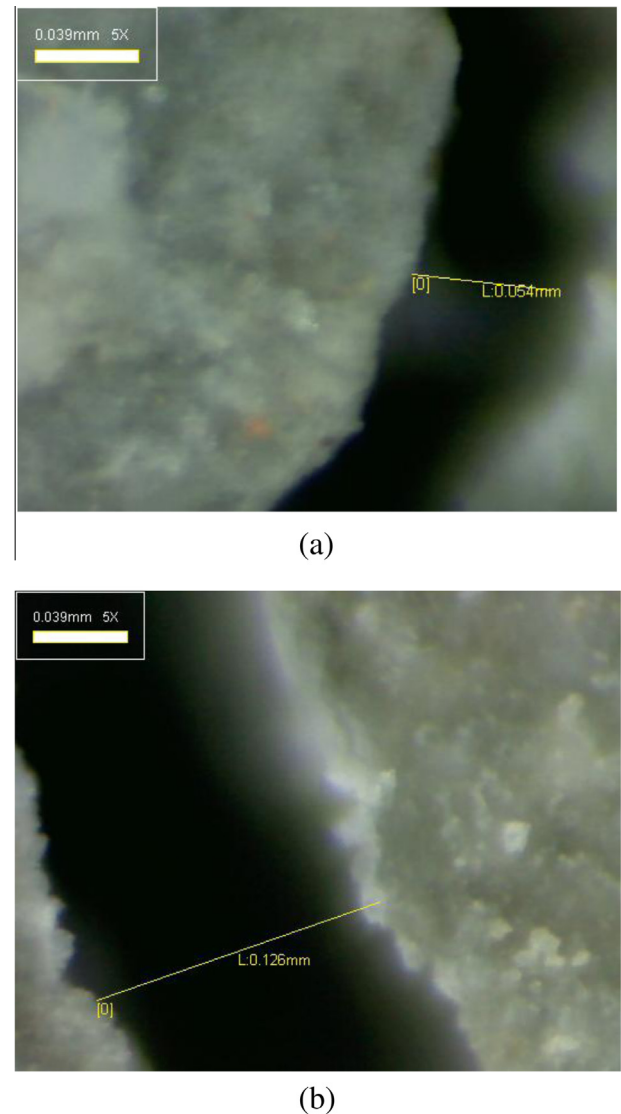


**Fig. 5.** Representative crack width: (a) S1.5 (crack width:  $0.054\ \text{mm}$ ) and (b) S1.0-PE0.5 (crack width:  $0.126\ \text{mm}$ ).

#### 4. Conclusions

This paper experimentally investigated the effect of combining 0.2 mm diameter straight steel fiber with microfibers on the mechanical properties of UHPC. A series of experimental tests were carried out to investigate various samples' mechanical properties and density. The following conclusions can be drawn from the current experimental results:

1. The S1.0-PE0.5, in which PE fiber was adopted instead of steel fiber for 33% of the total fiber volume, showed better tensile performance than steel fiber reinforced UHPC (S1.5). While the S1.0-PE0.5 showed 4.7% lower compressive strength, it showed 14% higher first cracking strength, 13% higher ultimate tensile strength and 39% higher tensile strain capacity than S1.5. On the other hand, the S1.0-PVA0.5 showed the worse tensile performance, i.e. lower first cracking strength, ultimate tensile strength, and tensile strain capacity, as compared to S1.5. It was found that the hybrid fiber system combining synthetic fiber with high strength and steel fiber can be adopted to improve the tensile behavior of UHPC.
2. While the S1.0-B0.5, in which basalt fiber was adopted instead of steel fiber for 33% of the total fiber volume, showed 14.1% lower compressive strength and 68% lower tensile strain capacity than S1.5, it showed 37% higher first cracking strength and 3% higher ultimate tensile strength than S1.5. It was found that the basalt fiber composed of minerals similar to that of cementitious materials is effective for improving the tensile strength of UHPC.
3. The density of S1.5 was 2.48 g/cm<sup>3</sup> and the densities of S1.0-B0.5, S1.0-PVA0.5, and S1.0-PE0.5 were relatively 2.0%, 1.6%, and 1.2% less, respectively. This decrease is attributed to the fact that microfiber has a lower density than steel fiber. From these test results, it was also confirmed that unintentional pores were not created by the microfiber addition.

#### Acknowledgments

This research was supported by a grant (13SCIPA02) from Smart Civil Infrastructure Research Program funded by Ministry of Land, Infrastructure and Transport (MOLIT) of Korea government and Korea Agency for Infrastructure Technology Advancement (KAIA).

#### References

- [1] ASCE. Report card for America's infrastructure; 2009.
- [2] Buitelaar P. Heavy reinforced ultra high performance concrete. In: Schmidt M, Fehling E, Geisenhanslüke C, editors. Proceedings of the international symposium on ultra high performance concrete. Kassel, Germany: Kassel University Press; 2004. p. 25–35.
- [3] Naaman AE, Wille K. The path to ultra-high performance fiber reinforced concrete (UHP-FRC): five decades of progress. In: Schmidt M, Fehling E, Glotzbach C, Fröhlich S, Piotrowski S, editors. Proceedings of Hipermat 2012 3rd international symposium on UHPC and nanotechnology for high performance construction materials. Kassel, Germany: Kassel University Press; 2012. p. 3–15.
- [4] Rossi P. Ultra high-performance concrete. *Concr Int* 2008;30(2):31–4.
- [5] Russel HG, Graybeal BA. Ultra-high performance concrete: a state-of-the-art report for the bridge community. McLean: Federal Highway Administration; 2013.
- [6] Association Française de Génie Civil, Ultra high performance fibre-reinforced concretes—Interim recommendations. Paris, France; 2002.
- [7] Japan Society of Civil Engineers. Recommendations for design and construction of high performance fiber reinforced cement composites with multiple fine cracks (HPFRCC). *Concr Eng Ser* 2008;82.
- [8] Li VC. Tailoring ECC for special attributes: a review. *Int J Concr Struct Mater* 2012;6(3):135–44.
- [9] Lee BY, Cho CG, Lim HJ, Song JK, Yang KH, Li VC. Strain hardening fiber reinforced alkali-activated mortar – a feasibility study. *Constr Build Mater* 2012;37:15–20.
- [10] Choi SJ, Choi JI, Song JK, Lee BY. Rheological and mechanical properties of fiber-reinforced alkali-activated composite. *Constr Build Mater* 2015;96:112–8.
- [11] Choi JI, Song KI, Song JK, Lee BY. Composite properties of high strength polyethylene fiber-reinforced cement and cementless composite. *Compos Struct* 2016;138:116–21.
- [12] Banthia N, Majdzadeh F, Wu J, Bindiganavile V. Fiber synergy in hybrid fiber reinforced concrete (HyFRC) in flexure and direct shear. *Cem Concr Compos* 2014;48:91–7.
- [13] Lawler JS, Wilhelm T, Zampini D, Shah SP. Fracture processed in hybrid fiber-reinforced mortar. *Mater Struct* 2003;36:197–208.
- [14] Lawler JS, Zampini D, Shah SP. Permeability of cracked hybrid fiber-reinforced mortar under load. *ACI Mater J* 2002;99(4):379–85.
- [15] Lawler JS, Zampini D, Shah SP. Microfiber and macrofiber hybrid fiber-reinforced concrete. *ASCE J Mater Civ Eng* 2005;17(5):595–604.
- [16] Park SH, Kim DJ, Ryu GS, Koh KT. Tensile behavior of ultra performance hybrid fiber reinforced concrete. *Cem Concr Compos* 2012;34(2):172–84.
- [17] ASTM. Standard specification for silica fume used in cementitious mixtures. ASTM C1240-14; 2014.
- [18] Roussel N. Understanding the rheology of concrete. Cambridge, UK: Woodhead Publishing Limited; 2012.
- [19] Li VC, Mishra DK, Wu HC. Matrix design for pseudo-strain-hardening fibre reinforced cementitious composites. *Mater Struct* 1995;28(10):586–95.
- [20] ASTM. Standard test method for compressive strength of hydraulic cement mortars (using 50 mm [2 in.] Cube Specimens). ASTM C109/C109M-07; 2007.
- [21] Kanda T, Li VC. Practical design criteria for saturated pseudo strain hardening behavior in ECC. *J Adv Concr Technol* 2006;4(1):59–72.
- [22] Choi JI, Lee BY. Bonding properties of basalt fiber and strength reduction according to fiber orientation. *Mater* 2015;8:6719–27.